Oligonucleotide Detection Using Angle-Dependent Light Scattering and Fractal Dimension Analysis of Gold−DNA Aggregates

Glauco R. Souza and J. Houston Miller*

Department of Chemistry
The George Washington University
Washington, DC 20052

Received December 22, 2000
Revised Manuscript Received May 25, 2001

As a result of recent biotechnological advancements, there is a great need for the development of affordable and sensitive instrumentation that can rapidly, quantitatively, and reproducibly[1] detect small variations in sequence and length of nucleic acids. Traditional techniques, such as gel electrophoresis, PCR (polymerase chain reaction), immunoassays, and membrane blots are inexpensive, but they are also time-consuming, often generate harmful wastes, and usually only provide either sequence or length of nucleic acids. This work applies a powerful but underutilized technique, angle-dependent light scattering[2] combined with fractal dimension[3] analysis (ADLS/FD), to detect the hybridization of Au−DNA nanoparticles to oligonucleotides of complementary sequence. We show that the ADLS/FD signal is uniquely sensitive to both concentration and length of an oligo-target. Further, this technique is well-suited for monitoring morphological changes during the fabrication of Au−DNA aggregates which are being proposed as building blocks for the construction of nanostructure architectures.[4]

The hybridization strategy used in this work is based on the principle first shown by Mirkin.[5] In their work, it was demonstrated that thiol-modified oligonucleotides covalently attached to gold nanoparticles (Au−DNA probe) hybridize to a target single-strand oligonucleotide of complementary sequence (oligo-target) in a liquid sample, forming a network of DNA and Au nanoparticles (Scheme 1). In Mirkin's work, UV−vis absorption of Au nanoparticles was used to detect DNA hybridization.

The ADLS apparatus (see Supporting Information) used in this work was constructed from off-the shelf optical components. Hybridization samples consisted of 0.1 pM of Au−DNA probe and oligo-target concentrations ranging from 0 to 2500 nM. The Au−DNA probes[6] consisted of 100 nm gold nanoparticles separately modified with either 3′- or 5′-end hexanethiol-functionalized oligonucleotide. The concentration of Au−DNA probes was determined by absorbance measurements at 575 nm using an extinction coefficient[7] of 1.62×10^{11} M^{-1} cm^{-1}. The oligo-targets[8] consisted of synthesized oligonucleotides of either 21 or 30 bases in length where the nine-base sequence on the 3′- and 5′-ends are complementary to the sequences of the Au−DNA probes. After samples were prepared, they were simultaneously put through three heat and cool cycles (Supporting Information) and incubated for 24 h at 4 °C.

Scheme 1

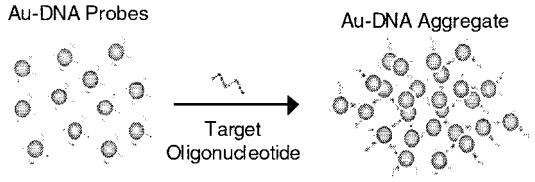

Researchers in the fields of material and combustion sciences have used ADLS and fractal dimension analysis in the study of structure and formation of colloidal and soot aggregates.[9,10] Fractal dimension can be defined as self-similar structures across scales.[2] We believe that an aggregate of Au−DNA nanoparticles assembled by the hybridization of Au−DNA probes to their oligo-target is a good example of fractal structure. Fractal theory[11] postulates that the relationship between the number of primary particles (N) in a fractal aggregate and its radius of gyration (Rg) obeys the relationship:[12]

$$N = \mathrm{kg}\left(\frac{\mathrm{Rg}}{a}\right)^{-\mathrm{Df}} \tag{1}$$

The angle-dependent light-scattering signal is related to the fractal dimension of an aggregate according to

$$NI(q) \approx \mathrm{kg}\cdot q(\theta)^{-\mathrm{Df}} \tag{2}$$

where $I(q)$ is the angle-dependent scattered light intensity, $q(\theta)$ is the scattering wavevector[13] which is a function of the scattering angle (θ) and wavelength of incident light (λ), and Df is the fractal dimension of the scattering aggregate. This relationship results from the interference between the scattered electromagnetic waves from the individual particles forming the fractal aggregate.[14]

Figure 1 shows the scattering signals for $30° \leq \theta \leq 150°$ for the Au−DNA hybridization with different concentrations of oligo-target. As the scattering intensity integrated across all angles increases with target concentrations, these results are consistent with literature results,[15] where UV−vis measurements have shown that extinction increases as a function of target concentration. As suggested above, analyses of the angle dependence of the scattering signal can be used to determine both Rg and Df and thus unveil details of the aggregate morphology. A Guinier plot [4a,16] allows the determination of the radius of gyration of an aggregate from the analysis of scattering intensity, $I(q)$, at low scattering angles. Under these conditions,

(1) (a) Cantor, C. R.; Cassandra, L. S. *Genomics: The Science and Technology Behind the Human Genome Project*; John Wiley & Sons: New York, 1999.
(2) Cohen, R. J.; Benedek, G. B. *Immunochemistry* **1975**, *12*, 349−51.
(3) Mandelbrot, B. B. *The Fractal Geometry of Nature*; Freeman, San Francisco, 1982.
(4) (a) Boal, A. K.; Ilhan, F.; DeRouchey, J. E.; Thurn-Albrecht, T.; Russell, T. P.; Rotello, V. M., *Nature* **2000**, *404*, 746−748. (b) Boal, A. K.; Rotello, V. M. *J. Am. Chem. Soc.* **1999**, *121*, 4914−4915.
(5) (a) Mirkin, C. A.; Letsinger, R. L.; Mucic, R. C.; Storhoff, J. J. *Nature* **1996**, *382*, 607−611. (b) Elghanian, R.; Storhoff, J. J.; Mucic, R. C.; Letsinger, R. L.; and Mirkin, C. A. *Science* **1997**, *277*, 1078−1081.
(6) 100 nm of Au particles (from BBI) modified with either 5′- or 3′-end hexanethiol modified oligonucleotide, $HS(CH_2)_6$-CCC-GCG-CCC-3′ and 5′-CCC-GCG-CCC-$(CH_2)_6SH$ respectively (Supporting Information).
(7) Yguerabide, J.; Yguerabide, E. E. *Anal. Biochem.* **1998**, *262*, 137−156.
(8) 5′-GGG-CGC-GGG-ATA-GGG-CGC-GGG-3′ or 5′-GGG-CGC-GGG-AAA-TAA-AAT-AAA-GGG-CGC-GGG-3′.
(9) (a) Stauffer, D. *Phys. Rep.* **1979**, *54*, 1−74. (b) Avnir, D.; Farin, D.; Pfeifer, P. *Nature* **1984**, *308*, 261−263.
(10) (a) Bryant, G.; Thomas, J. C., *Langmuir* **1995**, *11*, 2480−2485. (b) Thill, A.; Lambert, S.; Moustier, S.; Ginestet, P.; Audic, J. M.; Bottero, J. Y. *J. Colloids Interface Sci.* **2000**, *228*, 386-392. (c) Hyeon-Lee, J.; Beaucage, G.; Pratsinis, S. E. and Vemury, S. *Langmuir* **1998**, *14*, 5751−5756.
(11) (a) Koylu, U. O.; Faeth, G. M. *Trans. ASME* **1994a**, *116*, 971−979. (b) Martin, J. E.; Hurd, A. J. *J. Appl. Crystallogr.* **1987**, *20*, 61−78.
(12) a = mean primary particle radius, Df = fractal dimension, and kg = fractal prefactor.
(13) Valid for small scattering angles, $\mathrm{Rg}^{-1} \leq q(\theta) \leq a^{-1}$; $q(\theta) = (4\pi/\lambda)\sin(\theta/2)$.
(14) Mountain, R. D.; Mulholland, G. W. *Langmuir* **1988**, *4*, 1321−1326.
(15) Reynolds, R. A.; Mirkin, C. A.; Letsinger, R. L. *J. Am. Chem. Soc.* **2000**, *122*, 3795−3796.
(16) (a) Omotowa, B. A.; Keefer, K. D.; Kirchmeier, R. L.; Shreeve, J.M. *J. Am. Chem. Soc.* **1999**, *121*, 11130−11138. (b) Hunt, J. F.; McCrea, P. D.; Zaccai, G.; Engelman, D. M. *J. Mol. Biol* **1997**, *273*, 1004−1019. (c) Torre, J. G.; Harding, S. E.; Carrasco, B. *Biophys. J.* **1999**, *28*, 119−132.

10.1021/ja005919x CCC: $20.00
Published on Web 06/16/2001

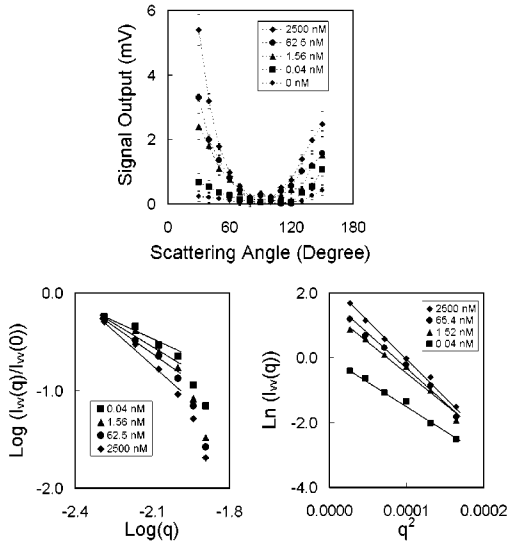

Figure 1. (Top) ADLS signal vs light-scattering angle for the hybridization of Au−DNA probes to different concentrations of 21-base long target. ADLS signal consisted of the raw scattering signal minus the background signal (scattering cell + hybridization buffer). (Bottom left) Fractal dimension analysis. ADLS data plotted as $\log(I_{vv}(q)/I_{vv}(0))$ vs $\log(q)$, $30° \leq \theta \leq 80°$. The linear regression analysis (lines) of each oligo-target concentration was done for θ ranging from $30° \leq \theta \leq 60°$ ($0.0034 \leq q(\theta) \leq 0.010$ nm^{-1}). (Bottom right) Guinier anlysis. Plot of the natural log of scattering intensity vs the square of the wavevector. The different data sets are the angle-dependent scattering intensity ($30° \leq \theta \leq 80°$) for the four different concentrations of target-oligo. The lines represent the linear fit for the low q region ($\theta \leq 70°$) of each data set.

$$I(q) \propto \exp\left(\frac{q(\theta)^2 \mathrm{Rg}^2}{3}\right) \tag{3}$$

Thus, Rg may be obtained from the slope of a plot of the natural logarithm of $I(q)$ as a function of the square of the scattering wavevector:

$$\mathrm{Rg} = \left[-3 \cdot \frac{\mathrm{d}(\ln(I(q)))}{\mathrm{d}(q^2)}\right]^{1/2} \tag{4}$$

The fractal dimension (Df) can also be extracted from the angle-dependent scattering data. From eq 2 it can be seen that the negative of the slope of the log of the normalized angle-dependent scattering signal versus the log of wavevector $q(\theta)$ yields the fractal dimension. This relationship is only valid at small angles (when $q(\theta) \leq 0.010$ nm^{-1}). Both the fractal dimension and Guinier analyses are shown in Figure 1.

Table 1 summarizes the results of the analyses performed on the data presented in Figure 1. Both the radius of gyration and the fractal dimension are found to be sensitive to target concentration. However, the latter shows a much greater sensitivity. The increase in aggregate density (as shown by the increase in Df with oligo-target concentration) is likely the outcome of increased intraparticle cross-linking at higher oligo-target concentration. The exponential dependence of the signal intensity on Df (eq 2) makes this method very sensitive and therefore ideal for detecting an oligo-target DNA fragment using Au−DNA probes.

The data of Figure 1 suggest that the morphology of the aggregates can be measurably altered by target concentration.

Table 1

target concentration (nM)	Rg (nm)	Df
0.04	215	1.3
1.56	245	1.6
62.5	251	1.9
2500	260	2.5

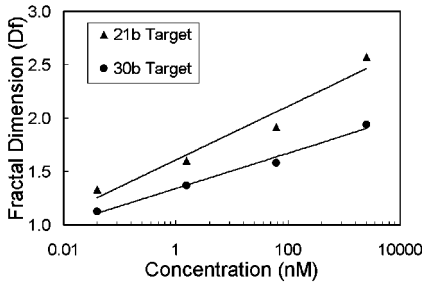

Figure 2. Df as a function of concentration of 21-base and 30-base long target oligonucleotides.

Figure 2 shows that the fractal dimension is also dependent on the length of the oligo-target, effectively increasing the spacing between the primary particles. To demonstrate this sensitivity, we compared the fractal dimension values for two systems with different oligo-target lengths: one in which the Au−DNA probe hybridizes to a 21-base long oligo-target, and the other in which the Au−DNA probe hybridizes to a 30-base long oligo-target. Each concentration of target showed lower Df values for the system containing the 30-base long oligo-target, in comparison to the one containing 21-base long oligo-target, indicative of more swollen and better solvated clusters[11b] for the former. Further, the increase in fractal dimension with concentration for both lengths of oligo-target further suggests a transition from string like aggregates (when Df is near unity) to denser, more compact structures at higher fractal dimesnion.[11b]

This study has illustrated the proof-of-concept of a technique that has the unique feature of simultaneously being sensitive to both concentration and length of a oligo-target. In addition, the presented apparatus consists of compact and inexpensive instrumentation, which could be readily incorporated into a portable instrument. Complementary techniques for determining aggregate structure, such as microscopy, require sample drying or other sample manipulations that can induce changes in the structure of these aggregates. Consequently, these techniques may produce results that do not reflect the actual structure of the Au−DNA aggregates in solutions. Finally, increasing attention has been paid to nanotechnology research, and more specifically, to using biological molecules as building blocks for building nanoscale structures. We feel that the methodology presented in this paper could be applied to the in situ analysis of nanostructure formation dynamics and morphology in a liquid environment.

Acknowledgment. We thank the Cosmos Club Foundation for supporting this work and KPL, Inc. for donating the molecular biology reagents and oligonucleotide probes. Additional support from the National Science Foundation and the National Institute of Standards and Technology is also gratefully acknowledged.

Supporting Information Available: ADLS apparatus; Au−DNA probes preparation; hybridization procedure (PDF). This material is available free of charge via the Internet at http://pubs.acs.org.

JA005919X